www.gi.sanu.ac.rs, www.doiserbia.nb.rs
J. Geogr. Inst. Cvijic. 2024, 74(3), pp. 291–309

Original scientific paper

UDC: 502.3:504.7(571.651)
https://doi.org/10.2298/IJGI2403291M

Received: September 12, 2024
Reviewed: November 2, 2024
Accepted: November 26, 2024

LONG-TERM EFFECT OF WARMING-INDUCED PERMAFROST THAWING ON TUNDRA VEGETATION—THE EVIDENCE FROM THE CHUKCHI PENINSULA (RUSSIAN NORTHEAST)

Alexey Maslakov[1]*, *Mikhail Grischenko*[1], *Alina Grigoryan*[1], *Dmitry Zamolodchikov*[2]

[1]Lomonosov Moscow State University, Faculty of Geography, Moscow, Russia; emails: alexey.maslakov@geogr.msu.ru; m.gri@geogr.msu.ru; aligrigoryan612@yandex.ru
[2]Russian Academy of Sciences, Center for Ecology and Productivity of Forests, Moscow, Russia; email: dzamolodchikov@hse.ru

Abstract: Tundra is one of the most sensitive environments of the world in relation to climate changes, since its ecosystems exist close to the limits of plant community tolerance. Besides, tundra vegetation in most of Arctic regions resides on permafrost, which is thermally unstable media. Thus, vegetation and frozen soils are extremely vulnerable to external impacts and are balancing in fragile thermodynamic equilibrium. Thermal and moisture regime shifting lead to changing of thermophysical properties of vegetation cover and thus, the thermal balance of underlying permafrost. In this study we present the results of 2001–2024 *in-situ* monitoring of vegetation cover and permafrost conditions in remote region of the Chukchi Peninsula, Russian Northeast. The study combines the yearly data on active layer thickness and vegetation cover from two sites of Circumpolar Active Layer Monitoring (CALM) program located within the key site of Eastern Chukotka Coastal Plains (ECCP). The study reveals long-term trajectories of climate, permafrost, and vegetation cover characteristics. Although common biological productivity was growing and active layer was thickening, the particular plant species respond to these changes differently. On sloping plots, the increasing of active layer thickness (ALT) led to correspondent lowering of the permafrost table, drainage of thawing ice and thus, soil drying, which caused the decrease in moss and sedge covers. Meanwhile, within flat poorly-drained surfaces the permafrost thawing contributes to soil moisture with correspondent sedge expansion. Thermokarst-affected terrain triggers the growth of tundra vegetation bioproductivity and serves as a shelter for plants from Arctic winds and facilitates higher snow accumulation.

Keywords: tundra; permafrost; climate change; Arctic; Chukotka

1. Introduction

Current climate changes are observed across the globe: global surface air temperatures have increased to 1.1 °C in 2011–2020 in comparison with pre-industrial period (IPCC, 2023). In the Arctic region climate shifts up to four times higher than global average (Rantanen et al., 2022). The observed trends have inevitable impact on the Arctic environment, affecting

*Corresponding author, e-mail: alexey.maslakov@geogr.msu.ru

its fragile balance. Numerous studies from different Arctic regions discover widespread permafrost degradation (Noetzli et al., 2023) and associated phenomena: increase of the active layer thickness (ALT), warming of the frozen rocks (Biskaborn et al., 2019; Kaverin et al., 2021; Strand et al., 2021), activation of thermokarst, thermal erosion (Farquharson et al., 2019), and thaw subsidence (O'Neill et al., 2023).

The vegetation in permafrost regions is both a sensitive indicator and a factor determining the conditions of heat exchange of the atmosphere and the underlying rocks (Tyrtikov, 1969). Vegetation and organic soil covers are as powerful regulator of permafrost conditions as climate (Anisimov et al., 2015; Guo et al., 2018). The evolution of vegetation cover as a result of climate warming can have a divergent effect on the depth of seasonal thawing of the soil and the temperature of permafrost rocks. The development of shrubby and woody vegetation can provoke positive feedback trapping more snow and thus, increasing soil temperature in winter (Laberge & Payette, 1995; Liston et al., 2002). On the other hand, growing shrubs shade the surface more strongly, reducing the temperature of the soil surface in summer (Frost et al., 2018). Thus, thermophysical properties of the upper soil and vegetation cover as well as surficial heat exchange conditions are important components of all current numerical permafrost models (Druel et al., 2017). For instatnce, Zhiltsova and Anisimov (2013) proposed an empirical-statistical model using bioclimatic indices to calculate the position of the boundaries of the main biomes under particular climate conditions. The use of such a model in conjunction with the analysis of the normalized difference vegetation index (NDVI) made it possible at the regional level to analyze the relationship of the biological productivity of Arctic natural zones with climatic characteristics and to forecast changes in vegetation cover.

Vegetation response to the changing permafrost and climatic conditions was also determined by organizing stationary (Moskalenko et al., 2014) and satellite (Stow et al., 2004; Varlamova & Soloviev, 2012) monitoring observations, as well as using numerical modeling. The interaction between vegetation and permafrost is an important factor determining the nonlinear response of ecosystems to climate change. Thus, the prediction of the response of vegetation to climate changes on decadal scale is problematic without considering the relationship between vegetation and permafrost (Lloyd et al., 2003). The issue of identifying such relationships is highlighted in phytoindication studies, which focused on searching for plant species, plant communities and their combinations, which serve as indicators of different natural processes (Ermokhina & Myalo, 2013; Lobotrosova et al., 2018).

The components of the environment that determine the functioning of plant communities are often related to climatic changes, which is most clearly observed in the Arctic. For example, the presence of the active layer and its thickness is closely related to the climate, and its warming may lead to an increase in the coverage of shrubs in tundra communities. Remote sensing methods revealed the movement of the forest-tundra boundary northward (Bhatt et al., 2013; Tishkov & Krenke, 2015) that was expressed in an increase in the average value of the NDVI over the past decades (Liu et al., 2024). The "greening" and "thickening" of the tundra also indicates the change of moss-lichen cover to grass-shrub cover, which, in turn, affects the conditions of freezing and thawing of soils (Myers-Smith et al., 2011; Tishkov et al., 2013).

The impact of global climate change on vegetation cover and its characteristics has a regional character. It depends on the specifics of climatic changes, which are expressed in

trends in temperature and precipitation indicators, and which differ significantly in space (Valentini et al., 2020). While western North America has a relatively high number of field vegetation studies on permafrost, Arctic tundra in Siberia is poorly studied (Heijmans et al., 2022). This study focuses on the region of Chukchi Peninsula, which is a remote northeastern part of Asia. Monitoring studies of vegetation and permafrost have been conducted here since the 2000s. These findings supported by weather station data and testimonies of local residents, reveal rapid change in the natural environment of the studied region. In this paper we present the evidence of long-term linkage between permafrost degradation and tundra vegetation cover shifts induced by regional climate variations.

2. Materials and methods

2.1. Study area

The Chuckhi Peninsula is the northeastern tip of Russia. This is one of the most inaccessible regions of the Russian Arctic. It is remote from both major logistics hubs and industrial centers, therefore the anthropogenic impact on its territory is limited to the presence of a dozen of indigenous communities. This area consists of flattened low mountains of the Mesozoic folding surrounded by the quaternary coastal plains (Figure 1).

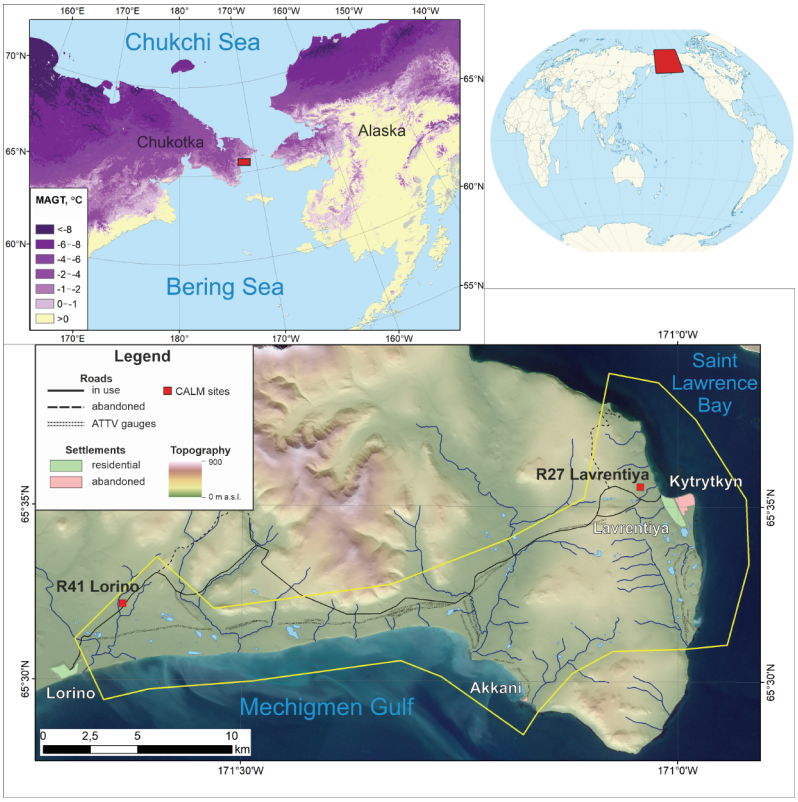

Figure 1. Eastern Chukotka Coastal Plains (ECCP) study area (outlined by yellow).

The subarctic marine climate determined the distribution of grass-shrub tundra vegetation on the plains and the lichen tundra and barrens in the mountains. The study area is characterized by a typical polar tundra climate type according to the Köppen–Geiger updated classification system (Kottek et al., 2006). The permafrost has continuous distribution with mean annual ground temperatures from –2 °C to –6 °C (Kolesnikov & Plakht, 1989). Permafrost landforms are presented by patterned grounds and kurums in mountain areas, thermokarst depressions and ice complex on plains and retrogressive thaw slumps in the coastal zone. Detailed natural conditions of the region are presented in Maslakov, Zotova, et al. (2021).

The key study site is named Eastern Chukotka Coastal Plains (ECCP). It covers an area of 172 km^2 and it is located between Lavrentiya and Lorino communities. The relief is presented mostly by fluvioglacial and marine plains and the adjacent low hills up to 300 m composed of weathered schists and granites. Although ECCP has been the key plot for permafrost and vegetation studies since 2019 (Maslakov, Egorov, et al., 2021; Maslakov, Zotova, et al., 2021), the permafrost monitoring of ALT was initiated in 2000 (Abramov et al., 2021; Zamolodchikov et al., 2004). Specific studies of transient layer of permafrost (Maslakov, Egorov, et al., 2021) and ground massive ice beds (Vasil'chuk et al., 2021) were organized to establish patterns of permafrost conditions in surficial sediments of the ECCP.

There are two monitoring sites within ECCP, established in the framework of Circumpolar Active Layer Monitoring (CALM) program (Brown et al., 2000): R-27 Laverntiya (since 2000) and R-41 Lorino (since 2010). They have 100 × 100 meters square-shapes and represent typical landscape conditions of the surrounding area.

Lavrentiya monitoring site is located 1.5 km NW from Lavrentiya village and occupies soft slope (2–3° to NE) surface between a barren ridge and fluvioglacial plain. Its absolute height is about 70 m. The surficial deposits are loams with boulders inclusion covered by thin peaty layer up to 20 cm in thickness. Over 70% the plot is occupied by sedges, 9% is covered by willow-sedge communities (*Carex aquatilis var. minor Boott, Salix arctica Pall., S. reticulata L.*) located predominantly on hummocks, and 6% is covered by forb-sedge communities. The rest of the area is open water. In general, the Lavrentiya site is characterized by a relatively low floristic diversity, which may be due to its location on a slope of fluvioglacial plain composed of loams.

Lorino site is located on poorly-drained marine-glacial terrace covered by peaty deposits up to 4 m thick. Approximately 70% of the site area is covered by sedges and 14% is open water surfaces. Dry plots are occupied by blueberries (*Vaccinium uliginosum subsp. uliginosum*), wild rosemary (*Rhododendron tomentosum Harmaja*) and birches (*Betula glandulosa Michx.*). These species are not typical of Lavrentiya, indicating a higher degree of microrelief development at the Lorino site, since the listed species grow mainly on hummocks. Sedge sphagnum communities and dwarf shrubs cover 3% and 2% of the plot, respectively. According to Circumpolar Arctic Vegetation Map (Raynolds et al., 2019), both CALM sites represent tussock-sedge, dwarf-shrub, moss tundra (G4) and sedge, moss, dwarf-shrub wetland (W2), covering almost 25% of ECCP area (Maslakov et al., 2019).

2.2. Climate and active layer data

Assessment of climate change impact on natural ecosystems is based on the idea that the conditions of existence of a particular biome are determined mainly by heat supply during the growing season, the severity of winters and moisture availability (Anisimov et al., 2011; Titkova & Vinogradova, 2015). Thus, climate and permafrost dynamics data were analyzed since early 2000s.

The measurements of ALT within both CALM monitoring sites are organized according to standard CALM protocol (Brown et al., 2000). Every site is a 100 × 100 meter grid with 121 measurement nodes, located 10 meters from each other. Thaw depth is defined by penetrating thawed ground by steel rod until permafrost table with accuracy of 1 cm. The measurements are conducted monthly during thawing period (June–September) to trace both intra-annual and inter-annual ALT dynamics. The maximum ALT of the year was measured in the September, while the ALT confined to vegetation peak cover was measured in late July.

Climate data were retrieved from the nearest weather station located in Uelen community (66°10'N, 169°50'W; WMO ID: 25399) 87 km north from ECCP. Daily temperature and precipitation data (AISPRI, 2024) were used to calculate the amount of precipitation and the sum of positive daily air temperatures for warm seasons of 2000–2023. The warm season is defined as a period with steady positive air temperatures. It corresponds to the period of soil thawing and active layer development; therefore, the sum of positive daily air temperatures is called Degree Days of Thawing (DDT; Nelson & Outcalt, 1987). This parameter corresponds well with ALT with different soil and vegetation conditions and is widely used in permafrost studies (Christiansen, 2004).

2.3. Methods to establish variability of vegetation cover at the local level

The composition of vegetation and plant abundance are recorded at the CALM sites annually from 2002 to 2023 in late July to early August, at the peak of vegetation, using the horizontal projection method. The following vegetation fractions are determined within the sites: *Salix* spp., *Rubus chamaemorus* L., *Vaccinium vitis-idaea* L., *Empetrum nigrum* L., *Carex* spp., *Carex* spp. (dry), *Petasites frigidus* (L.) Fr., *Sphagnum* spp., other vascular plants, other mosses, and lichens (various). Due to the larger plant diversity, additional species are identified at Lorino site: *Rhododendron tomentosum* Harmaja, *Betula glandulosa* Michx., and *Vaccinium uliginosum* L. The projective cover of the above mentioned plant species/genera is calculated at each grid node with special 40 × 40 cm frames (121 calculations for each CALM site). The frame grid is divided into parts reflecting 50, 25, 16, 5, 4 and 1% of its area, which allows for sufficiently objective and reliable determination of the projective cover of plants, as well as the analysis of their ratio. Data collection for CALM-Lavrentiya has been conducted since 2002, and for Lorino since 2013, which makes it possible to assess the long-term dynamics of the vegetation cover. Collected data are presented in Tables 3a and 3b.

The trends of long-term observations data (vegetation, ALT and weather parameters) were calculated in MS Excel software using least squares method. The trend line type (linear, polynomial, etc.) choice was determined by the maximum determination coefficient (R^2).

2.4. Calculation of NDVI for ECCP

To find the most representative images covering the study area on the Chukotka Peninsula, it was necessary to determine the period of the peak of vegetation for each of the years under consideration. To solve this problem, low-resolution NDVI index images presented on the EarthExplorer portal were analyzed. The peak of vegetation was taken to be the dates that corresponded to the maximum NDVI values for each year from 2000 to 2023 within the ECCP.

For 2002–2022, the portal archive contains products with the NDVI index calculated from images of the MODIS sensor of the Terra satellite. However, for 2000 and 2001 only the data from the NOAA-14 meteorological satellite was found. To analyze the peak of vegetation

activity in 2023, the products of the EROS satellite (VIIRS sensor) were used, since the portal does not have images of the MODIS sensor obtained after October 1st, 2022. Each image contains the vegetation index values averaged over six days; images for 2023 are formed similarly to the MODIS sensor images, showing NDVI values averaged over every six days. The use of such averaged index images is the most convenient for assessing the interannual variability of vegetation activity.

As expected, the average peak of vegetation in the study area occurs at the end of July – beginning of August. However, inter-annual variability was detected: the dates of the peak of vegetation activity in the period from 2000 to 2023 can vary from July 15–21 to August 13–19 (Table 1a). For each year, Landsat satellite images covering the territory of ECCP were selected. Landsat 7 images are available for all required years, Landsat 8-9 satellite images are available for 2013 and later. Landsat-5 satellite images available for 2005–2008 and 2010–2011 were also considered. Thus, the number of available images varies both for the vegetation period and for the days corresponding to the peak of vegetation (Table 2a).

Since most of the images were taken under very high cloud cover (Table 2a), it was not possible to find cloud-free images taken during the peak of vegetation for the particular years. No cloud-free images were found for 2001, 2014, 2017, and 2020. More than 60% of all the selected images (15 out of 24) correspond to the identified vegetation peaks by date or were taken within three days from its beginning or end. Two more images differ from the vegetation peak by no more than six days (2017 and 2023). Finally, in seven cases, it was not possible to find cloud-free images for dates close to the peak of vegetation activity; the difference in the date of surveying the area and the onset of the peak ranges from 10 days to three weeks.

3. Results

3.1. Active layer thickness, air temperature, and precipitation variability

The warm season on Chukchi Peninsula usually lasts from the beginning of June till the end of September. Figure 2 presents the dynamics of the sum of positive daily temperatures by the peak of vegetation and for the whole warm season for 2001–2022. Although there is large amplitude between warm and cold summers (min. 401 °C, max. 1027 °C), there are no significant interannual trends. However, the warm and cold waves are clearly distinguished on the graph. Warm periods with accumulated DDT over 700 °C are 2002–2007 and 2014–2020; cold periods with DDT under 700 °C are 2008–2013 and 2021–2022 (continuing till 2024). The precipitation amount varies significantly from year to year. The driest summer was observed in 2018, with only 10 mm of precipitation; in contrast, 130 mm of precipitation was observed in 2021. Although there is an uplifting trend on summer precipitation amount (Figure 2), its interannual variability does not allow to state about its statistical significance.

It is noteworthy that although current weather characteristics have no directed trends since 2000s, there is clear warming for this territory, observed since 1950s (Maslakov et al., 2020). Mean annual air temperatures have been increasing since that time by 0.6–0.7 °C per decade with recent acceleration to 1.1–1.2 °C per decade since 1990s. These changes are contributed mostly by increasing of winter air temperatures. However, summer thermal conditions have also changed significantly: average accumulated DDT for 1950–1970 for Uelen weather station was 498 °C, while for 2000–2020 it was 704 °C. Thus, since the middle of the 20th century, summers on the Chukchi Peninsula have become warmer by 30%, which had effects both on permafrost and vegetation conditions.

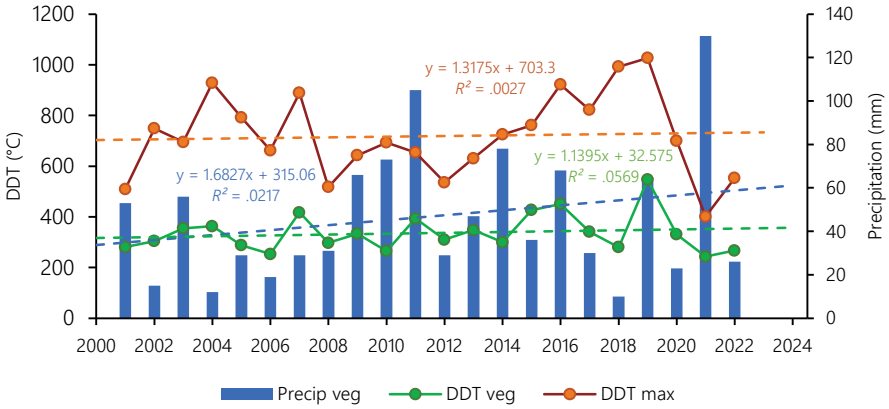

Figure 2. The variations of accumulated sum of precipitation for peak of vegetation (Precip veg), sum of positive air temperatures for peak of vegetation (DDT veg), and for the whole warm season (DDT max) for 2001–2022 at Uelen weather station.
Note. Dashed lines are linear trends with correspondent equations and determination coefficients.

The results of the ALT measurements are shown in Figure 3. Maximal seasonal thawing depth for Lavrentiya CALM site vary from 59 to 78 cm, while for Lorino interannual variations they are 47–66 cm. The linear trends for both sites are uplifting. However, for the recent four years (2021–2024) ALT decreases drastically.

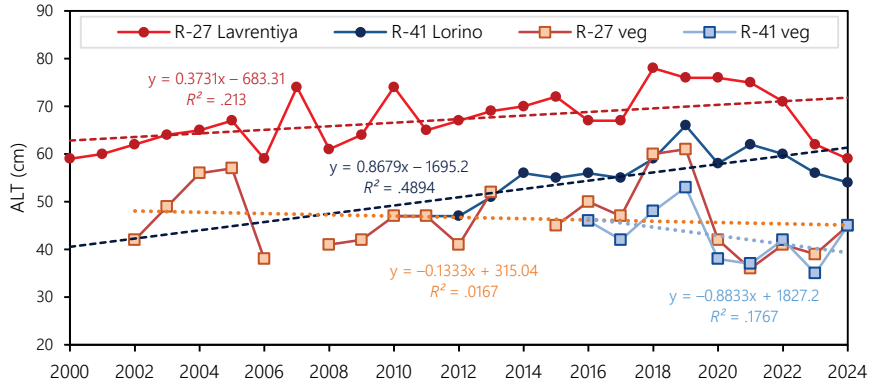

Figure 3. Active layer thickness dynamics on Lavrentiya and Lorino CALM sites for 2000–2024.
Note. Dashed lines are linear trends with correspondent equations and determination coefficients. The orange and blue lines "R-27 veg" and "R-41 veg" represent ALT dynamics confined to vegetation activity peak (late July–early August) for Lavrentiya and Lorino CALM sites, respectively.

The warm and cold waves noted in Figure 2 are also reflected in ALT dynamics for both CALM sites. The correlation coefficient (*R*) between ALT and DDT square root for both sites is .81–.83, which reveals good consistency between summer thermal characteristics and soil thaw depth. This is a common pattern for many other CALM sites from all over the world

(Kaverin et al., 2021). The thaw depths variations confined to vegetation peak are also represented on Figure 3 (R-27 veg and R-41 veg). The linear trends for both CALM sites are negative, but statistically insignificant (p > .05). Apparently, there is no notable long-term dynamics is vegetation peak ALT, while maximal ALT is following summer thermal waves with slightly increasing long-term trend.

3.2. Vegetation variability within CALM sites

In order to avoid subjective distortions, the projective cover analysis was performed for 2013–2024. The average total projective cover within CALM sites during 2013–2024 is 48% for Lavrentiya site and 67% for Lorino. The maximum projective vegetation cover (excluding dry sedges) for Lavrentiya was about 68–74% and it was detected in 2015–2016, while for Lorino site it was 67% in 2018 (Figure 4). Minimal vegetation cover extent was detected in 2023–2024 for both sites (38–40%). Thus, extreme values of total vegetation cover correspond to summer thermal waves (Figure 2).

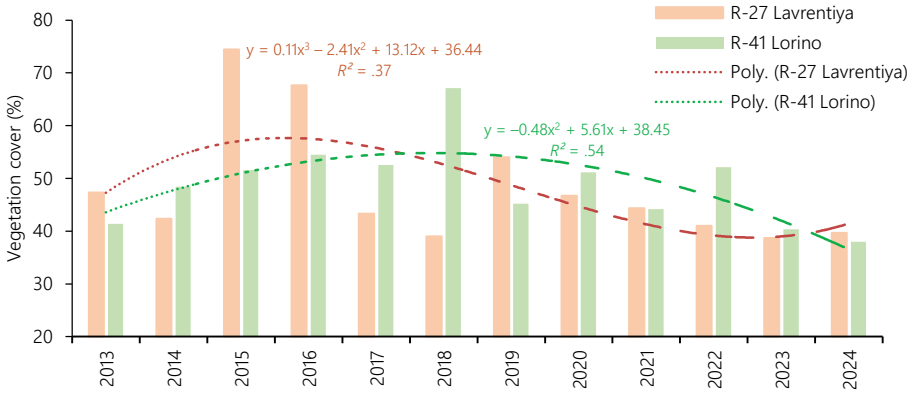

Figure 4. Projective cover within CALM sites of ECCP.

The long-term variations of the projective cover of particular plants or their groups were considered for both CALM sites. The years with data that significantly deviates from the average values (in several times within adjacent years) were excluded from the analysis as distorted by subjective assessment.

The year-to-year variations of predominant plant species/genera for both CALM sites are shown in Figures 5 and 6. Significant decrease in the projective cover of sedges was revealed within Lavrentiya site (Figure 5), while shrinking of willows cover was detected only for 2002–2007 with further stabilization. Sphagnum cover variations are fragmented, but well fit within the 2nd polynomial trend (R^2 = .95) with the period of shrinking cover in 2005–2012, minimal extent in 2012–2017, and then expanding in 2017–2024. The rest of plant species occupy minor spaces and did not represent significant changes.

For Lorino site predominant plant species/genera demonstrate divergent trends in projective cover. Thus, sedges cover is slightly increasing, while lichens are shrinking with statistically significant trend. The projective cover area of dwarf birch (*Betula glandulosa* Michx.) may serve as a good indicator of heat supply since it has good correspondence with

2nd polynomial trend demonstrating its highest values for 2016–2020, which coincides with warm wave. The crowberry (*Empetrum nigrum* L.), cowberry (*Vaccinium vitis-idaea* L.), blueberry (*Vaccinium uliginosum* L.), and wild rosemary (*Rhododendron tomentosum Harmaja*) combined into evergreen shrubs, as well as cloudberry (*Rubus chamaemorus* L.) and sphagnum covers did not express significant changes (Figure 6).

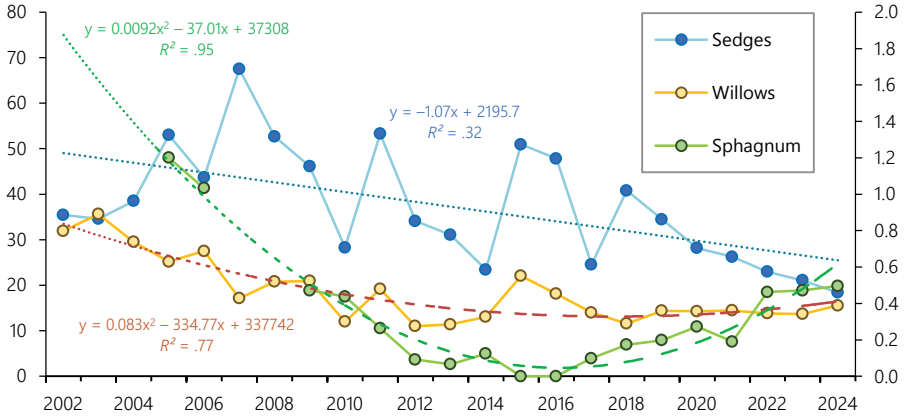

Figure 5. Variations of vegetation cover of predominant plant species/genera within Lavrentiya site (%).
Note. Data for Sphagnum is given for secondary axis.

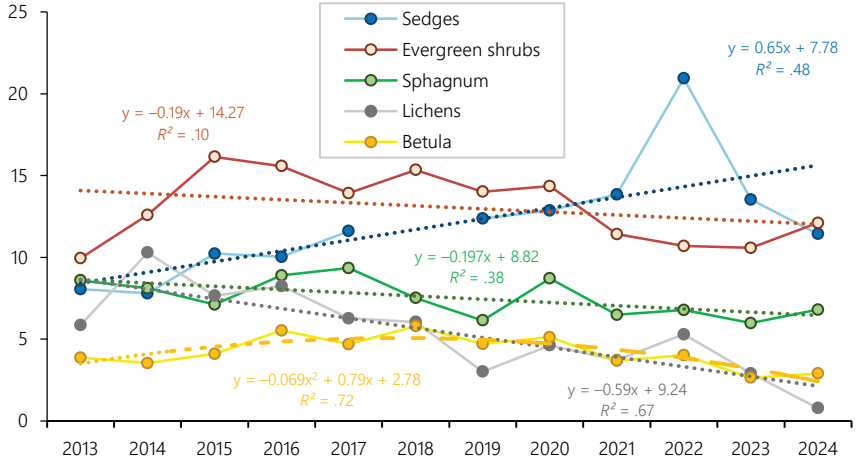

Figure 6. Variations of vegetation cover of predominant plant species/genera within Lorino site (%).

3.3. Changes of NDVI for 2001–2023

The results of calculating the NDVI values are presented in Table 3a. The results for 2001 and 2017 are significantly out of the range since these images are characterized by high cloud coverage. Therefore it was not possible to correctly calculate the NDVI values from them. The standard deviation values of NDVI are .15 ± .03, which indicates the comparability of the obtained results.

The long-term variability of the average NDVI values is shown in Figure 7. In addition to high cloud cover issue, the NDVI calculation results were also affected by some images with dates being too early or too late relative to the vegetation peak (Tables 1a, 2a). Thus, the image date differs from the vegetation peak by more than six days for 2010 and 2020 (too late) and for the period 2012–2014 (too early). These data were excluded from further analysis. Figure 7 shows a general upward trend in NDVI with R^2 = .46. In less timescale, a slight downward trend in NDVI values was noted in 2005–2014, which was then replaced by an upward trend in 2014–2023, which generally coincides with revealed summer heat and cold waves (Figure 2).

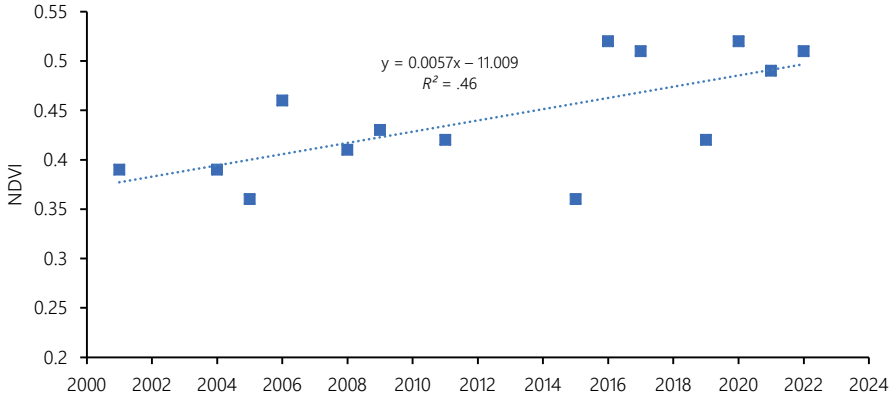

Figure 7. Variability of NDVI values calculated from Landsat satellite images for ECCP.

4. Discussion

4.1. Permafrost and vegetation interaction within CALM sites

As shown in Figure 2, the variations in temperature and precipitation of the summer seasons are divided into short-term heat and cold waves. The latter include seasons with high precipitation, such as 2010, 2011, and 2021. The variations in summer heat and moisture conditions are reflected in changes in the projective cover of vegetation at the CALM sites. Thus, the total projective cover of vegetation (Figure 4) had been increasing until the summer of 2018, and then gradually decreasing from 2019, recording its highest values during the period of the warm summers.

The detailed analysis of the projective cover variations of particular vegetation species revealed local differences in the moisture and heat supply conditions at both CALM sites. Thus, the Lavrentiya site is characterized by decreasing in coverage of mosses acting as moisture indicator in 2005–2013, followed by its expanding in 2016–2024. At the same time, hydrophilic sedges also showed the decrease in projective coverage from 2005 to 2024, i.e., during almost the entire observation period. The dynamics of the projective covering of willows, which depend rather on air temperature than on humidification, shows a slight decrease in this indicator in 2002–2011, and then the absence of significant trends until 2024. Another confirmation of gradual soil desiccation is the variation of dry sedges coverage, which demonstrates a remarkably increasing trend (Figure 8). Until the summer of 2008, dry sedges cover was slightly decreasing, and after that it was a steadily increasing. At the same

time, the maximum depth of seasonal soil thawing had been increasing continuously from 59–65 cm in 2001–2004 up to 75–78 cm in 2018–2021 (Figure 3), despite the absent long-term trends in DDT variations (Figure 2). Considering the location of CALM Lavrentiya site on a gentle slope, melted ground ice from the foot of the active layer and transient layer of permafrost drained downhill, leading to irreversible surface settlement (Maslakov et al., 2019). The gradual lowering of the permafrost table, which serves as local waterproof level, contributed to the desiccation of the upper soil layer.

Thus, the phytoindication features combined with the ALT monitoring results, demonstrate a long-term stable trend towards decreasing of soil moisture at CALM Lavrentia site from approximately the mid-2000s to the present. At the same time, short-term heat and cold waves in summer periods correct this trend. From approximately 2010 to 2018, a slight decrease in moisture was noted, which is manifested in a decrease in the projective cover of mosses and an increase in the proportion of dry sedges at the site. Since 2018, a simultaneous decrease in the heat supply of the summer period from 900–1000 °C to 400–500 °C and an increase in the amount of summer precipitation have been observed, which is reflected in a further decrease in the projective cover of sedges and an expansion of the moss cover area.

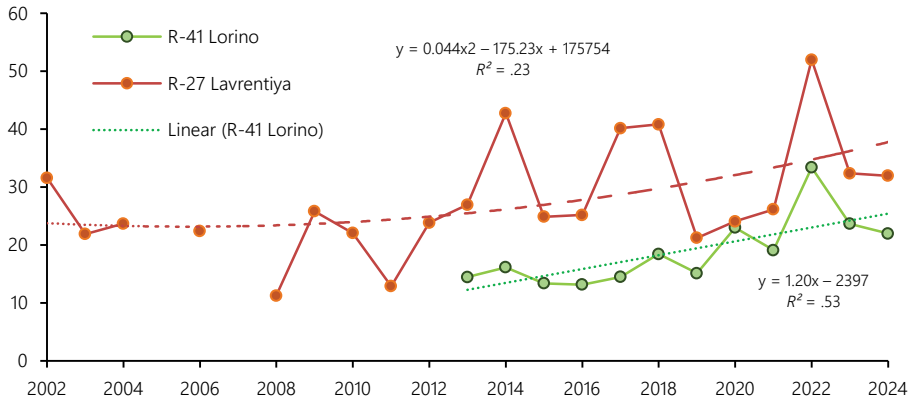

Figure 8. Variations of dry sedges cover (%) for Lavrentiya and Lorino CALM sites.

Unlike Lavrentiya, Lorino CALM site is located on a poorly drained surface with peaty soils and a developed hummocky microrelief. Despite the higher ALT increasing rate here, the shorter observation period (2013–2024) does not allow us to confidently identify distinct long-term trends in vegetation cover of particular plants. The most pronounced trend is represented by lichen cover shrinking, which may be interpreted as the increase of soil moisture. However, the coverage of sphagnum, serving as indicator of increased soil moisture, is also slightly decreasing. Only sedges and dry sedges projective covers have demonstrated the increase for the observed period. Overall, in poorly-drained Lorino site environment the processes of permafrost degradation did not lead to noticeable soil desiccation. Melted ice from the transient layer of permafrost contributes to soil moisture. Besides, increased active layer may facilitate better soil conditions for biological activity and plant roots development. In this case, the permafrost degradation is a rather positive factor for biological productivity of plants. Similar results were noticed at the islands of High Arctic

(Mikhailov, 2020), where degradation of ice complex leads to different trajectories of the vegetation development depending on draining conditions.

4.2. NDVI variations and in-situ vegetation studies

The calculated NDVI values at the peak of vegetation clearly demonstrate a long-term upward trend. Even despite the relatively cool (both dry and rainy) summer seasons of 2020–2022, accompanied by ALT thinning, bioproductivity was higher than in the relatively warm seasons of 2004–2007. This pattern allows us to assume that another factor that affects bioproductivity. In our opinion, this is the factor of degrading permafrost.

On one hand, on sloping and well-drained areas (such as CALM Lavrentiya) the increase of ALT leads to correspondent lowering of the permafrost table and drainage of melted ice. On the other hand, on flat surfaces (such as CALM Lorino) the ice thawing from the transient layer contributes to soil moisture. Such contribution is more expressed in a dry summer season, e.g., 2020, when low precipitation amount, combined with average DDT value resulted in the highest value of NDVI for the observed period. In the neighboring region of the Seward Peninsula (Alaska, the U.S.) the study of ALT and drainage conditions effect on vegetation revealed that warming-induced tree and shrubs propagation is limited by the availability of well-drained microsites (Lloyd et al., 2003). Based on these findings, we suppose that further climate warming will facilitate intensive shrub development on well-drained sites such as drainage channels and hollows banks.

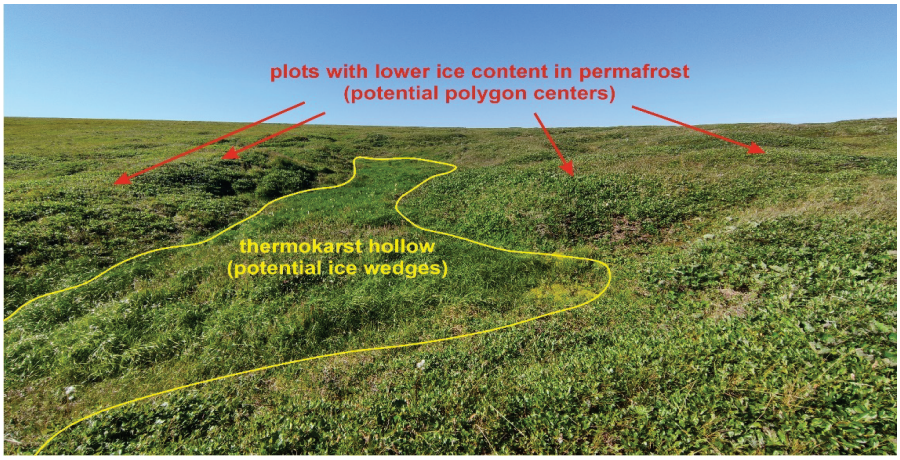

Figure 9. Thermokarst affected terrain, located 3 km south from Lavrentiya community.
Note. The hollow is covered with dense sedges cover and surrounded by hills, covered with willows.

Besides, observed active layer thickening causes widespread thermokarst and thaw subsidence development, observed in different permafrost regions in common and in ECCP, in particular. We do not have quantitative assessment of areas experiencing these processes or its velocity, but some preliminary observations make us conclude that plots with thermokarst-affected terrain have higher grasses and more diverse plant communities than in flat undisturbed surfaces (Figure 9). In this case, differentiated relief serves as a shelter for plants from Arctic winds and facilitates higher snow accumulation. The revealed patterns in

common correspond to the field reports from other regions of the Arctic (Heijmans et al., 2022). The obtained results are in line with the recently published global studies of ALT and NDVI correspondence (Yang et al., 2024). Weak positive trends in NDVI and ALT are characteristic for the whole Northeastern Asia region. Besides, for the tundra environments temperature changes have higher influence on vegetation greening than precipitation does.

4.3. Predicted estimations of permafrost and vegetation evolution in the 21st century

According to estimations of CMIP6 simulations (IPCC, 2023), the global air temperatures increase will reach 1.0–5.7 °C by 2080–2099. For the Arctic latitudes, these values may be twice or triple higher. In this case, the ongoing permafrost thawing trends will continue. According to our previous estimations (Maslakov et al., 2019), ALT in Chukchi Peninsula will increase by the end of the 21st century up to 87% from current values. The melting ice from the transient layer of permafrost will facilitate soil surface lowering with rates of 0.4–3.7 cm. Total soil subsidence will vary from 50 to 250 cm, depending on climate scenario. Our estimations are higher than recent results obtained from North Alaska (Painter et al., 2023; Wang et al., 2023) since we used simple empirical model disregarding ice distribution in permafrost section and the effect of drying of tundra landscapes.

The mentioned changes will lead to a profound shifting of the vegetation structure of Chukchi Peninsula. We assume that climate warming will cause abrupt permafrost thaw and consecutive thermokarst and thermal erosion landforms development. Deepening of hollows and ravines in sloping areas will contribute to further soil desiccation and thus, the development of shrub and appearance of tree cover in these environments, mostly represented by willows. Similar processes have been observed on Seward Peninsula located 150 km to the east from ECCP (Lloyd et al., 2003). Within poorly drained plots, a lush growth of sedges is expected without changing of vegetation structure. Besides, we expect the boundaries of altitudinal vegetation zones to grow. However, the quantity estimations of expected changes are unclear due to the lack of current observation data in this region.

5. Conclusion

In this paper we considered long-term variations of weather parameters, active layer thickness, and vegetation cover in remote Arctic site of ECCP (Chukchi Peninsula, Russian Northeast). The vegetation cover was assessed both from satellite imagery and from in-situ field monitoring. Our studies revealed complex interactions between vegetation and degrading permafrost on the background of climatic shifts:

- Air temperature in Chukchi Peninsula region had been increasing since the 1950s resulting in doubling of summer heat supply in 2000–2020 in comparison with 1950–1970. In the last decades short-term variations were observed: warm periods were 2002–2007 and 2014–2020; cold periods were 2008–2013 and 2021–2024. Summer precipitation amounts varied significantly from year to year and did not reveal long-term patterns;
- Observed climate changes affected permafrost conditions facilitating ALT thickening with average rates of 0.3–0.9 cm per year. Permafrost thawing leads to the increase of terrain dissection and formation of thermoerosional and thermokarst landforms. These tendencies have consecutive effects on tundra vegetation cover;
- On sloping areas, such as CALM Lavrentiya site, the increase of ALT for the last 23 years led to the correspondent lowering of the permafrost table, drainage of thawing ice and

thus, soil drying. It caused the decrease of moss and sedge covers and increase of the ratio of dry sedges;

- On flat poorly-drained surfaces, such as CALM Lorino site, the ice melting from the transient layer does not drain completely and contributes to soil moisture, especially in dry summer seasons; and
- Commonly, permafrost degradation, combined with summer warming, has positive effects on the increase of biological productivity of tundra plant communities. In addition to extra moisture from thawing transient layer, thermokarst-affected terrain serves as a shelter for plants from Arctic winds, facilitates higher snow accumulation and creates conditions for shrubs growing on drained soils.

Acknowledgements

This study was supported by RSF grant 23-77-01016 "The transformation of cryogenic environment of Chukotka coastal plains due to climate change". Long-term field studies were supported by U.S. National Science Foundation awards OPP1304555 and 1836377.

References

Abramov, A., Davydov, S., Ivashchenko, A., Karelin, D., Kholodov, A., Kraev, G., Lupachev, A., Maslakov, A., Ostroumov, V., Rivkina, E., Shmelev, D., Sorokovikov, V., Tregubov, O., Veremeeva, A., Zamolodchikov, D., & Zimov, S. (2021). Two decades of active layer thickness monitoring in northeastern Asia. *Polar Geography*, *44*(3), 186–202. https://doi.org/10.1080/1088937X.2019.1648581

AISPRI. (2024). Specializirovannyi massivy dlya klimaticheskih issledovanij [Automated Information System for Processing Regime Information, Data set]. http://aisori-m.meteo.ru/waisori/index.xhtml?idata=19

Anisimov, O. A., Zhiltsova, E. L., & Reneva, S. A. (2011). Estimation of critical levels of climate change influence on the natural terrestrial ecosystems on the territory of Russia. *Russian Meteorology and Hydrology*, *36*, 723–730. https://doi.org/10.3103/S1068373911110033

Anisimov, O. A., Zhirkov, A. F., & Sherstyukov, A. B. (2015). Sovremennyye izmeneniya kriosfery i prirodnoy sredy v Arktike [Current changes in cryosphere and environment in the Arctic]. *Arctic XXI century, 2*(3), 24–47. https://cyberleninka.ru/article/n/sovremennye-izmeneniya-kriosfery-i-prirodnoy-sredy-v-arktike

Biskaborn, B. K., Smith, S. L., Noetzli, J., Matthes, H., Vieira, G., Streletskiy, D. A., Schoeneich, P., Romanovsky, V. E., Lewkowicz, A. G., Abramov, A., Allard, A., Boike, J., Cable, W. L., Christiansen, H. H., Delaloye, R., Diekmann, B., Drozdov, D., Etzelmuller, B., Grosse, G., . . . Lantuit, H. (2019). Permafrost is warming at a global scale. *Nature Communications*, *10*(1), Article 264. https://doi.org/10.1038/s41467-018-08240-4

Bhatt, U. S., Walker, D. A., Raynolds, M. K., Bieniek, P. A., Epstein, H. E., Comiso, J. C., Pinzon, J. E., Tucker, C. J., & Polyakov, I. V. (2013). Recent Declines in Warming and Vegetation Greening Trends over Pan-Arctic Tundra. *Remote Sensing, 5*(9), 4229–4254. https://doi.org/10.3390/rs5094229

Brown, J., Hinkel, K. M., & Nelson, F. E. (2000). The circumpolar active layer monitoring (CALM) program: research designs and initial results. *Polar Geography, 24*(3), 166–258. https://doi.org/10.1080/10889370009377698

Christiansen, H. H. (2004). Meteorological control on interannual spatial and temporal variations in snow cover and ground thawing in two northeast Greenlandic Circumpolar-Active-Layer-Monitoring (CALM) sites. *Permafrost and Periglacial Processes, 15*(2), 155–169. https://doi.org/10.1002/ppp.489

Druel, A., Peylin, P., Krinner, G., Ciais, P., Viovy, N., Peregon, A., Bastrikov, V., Kosykh, N., & Mironycheva-Tokareva, N. (2017). Towards a more detailed representation of high-latitude vegetation in the global land surface model ORCHIDEE (ORC-HL-VEGv1.0). *Geoscientific Model Development, 10*(12), 4693–4722. https://doi.org/10.5194/gmd-2017-65

Ermokhina, K. A., & Myalo, E. G. (2013). Fitoindikacionnoe kartografirovanie opolznevyh narushenij na Central'nom Yamale [Phytoindication mapping of landslide disturbances in the Central Yamal]. *Izvestiya Rossiiskoi Akademii Nauk. Seriya Geograficheskaya, 5,* 139–146. https://izvestia.igras.ru/jour/article/view/99

Guo, W. C., Liu, H. Y., Anenkhonov, O. A., Shangguan, H., Sandalov, D. V., Korolyuk, A. Y., Hu, G., & Wu, X. (2018). Vegetation can strongly regulate permafrost degradation at its southern edge through changing surface freeze-thaw processes *Agricultural and Forest Meteorology, 252,* 10–17. https://doi.org/10.1016/j.agrformet.2018.01.010

Heijmans, M. M. P. D., Magnússon, R. Í., Lara, M. J., Frost, G. V., Myers-Smith, I. H., van Huissteden, J., Jorgenson, M. T., Fedorov, A. N., Epstein, H. E., Lawrence, D. M., & Limpens, J. (2022). Tundra vegetation change and impacts on permafrost. *Nature Reviews Earth & Environment*, *3*, 68–84. https://doi.org/10.1038/s43017-021-00233-0

IPCC (2023). *Climate Change 2023: Synthesis Report. Contribution of Working Groups I, II and III to the Sixth Assessment Report of the Intergovernmental Panel on Climate Change*. IPCC. https://doi.org/10.59327/IPCC/AR6-9789291691647

Farquharson, L. M., Romanovsky, V. E., Cable, W. L., Walker, D. A., Kokelj, S. V., & Nicolsky, D. (2019). Climate Change Drives Widespread and Rapid Thermokarst Development in Very Cold Permafrost in the Canadian High Arctic. *Geophysical Research Letters, 46*(12), 6681–6689. https://doi.org/|10.1029/2019GL082187

Frost, G. V., Epstein, H. E., Walker, D. A., Matyshak, G., & Ermokhina, K. (2018). Seasonal and Long-Term Changes to Active-Layer Temperatures after Tall Shrubland Expansion and Succession in Arctic Tundra. *Ecosystems, 21,* 507–520. https://doi.org/10.1007/s10021-017-0165-5

Kaverin, D., Malkova, G., Zamolodchikov, D., Shiklomanov, N., Pastukhov, A., Novakovskiy, A., Sadurtdinov, M., Skvortsov, A., Tsarev, A., Pochikalov, A., Malitsky, S., & Kraev, G. (2021). Long-term active layer monitoring at CALM sites in the Russian European North. *Polar Geography, 44,* 203–216. https://doi.org/10.1080/1088937X.2021.1981476

Kolesnikov, S. F., & Plakht, I. R. (1989). Chukotskij rajon [Chukotka Area]. In A. I. Popov (Ed.), *Regional'naya Kriolitologiya* [Regional Cryolithology] (pp. 201–217). MGU.

Kottek, M., Grieser, J., Beck, C., Rudolf, B., & Rubel, F. (2006). World Map of the Köppen-Geiger climate classification updated. *Meteorologische Zeitschrift*, *15*(3), 259–263. https://doi.org/10.1127/0941-2948/2006/0130

Laberge, M.-J., & Payette S. (1995). Long-Term Monitoring of Permafrost Change in a Palsa Peatland in Northern Quebec, Canada: 1983–1993. *Arctic and Alpine Research, 27*(2), 167–171. https://doi.org/10.2307/1551898

Liston, G. E., McFadden, J. P., Sturm, M., & Pielke, R. A. (2002). Modelled changes in arctic tundra snow, energy and moisture fluxes due to increased shrubs. *Global Change Biology, 8*(1), 17–32. https://doi.org/10.1046/j.1354-1013.2001.00416.x

Liu, Z., He, D., Shi, Q., & Cheng, X. (2024). NDVI time-series data reconstruction for spatial-temporal dynamic monitoring of Arctic vegetation structure. *Geo-spatial Information Science*, 1–19. https://doi.org/10.1080/10095020.2024.2336602

Lloyd, A. H., Yoshikawa, K., Fastie, C. L., Hinzman, L., & Fraver, M. (2003). Effects of permafrost degradation on woody vegetation at arctic treeline on the Seward Peninsula, Alaska. *Permafrost and Periglacial Processes, 14*(2), 93–101. https://doi.org/10.1002/ppp.446

Lobotrosova, S. A., Soromotin, A. V., Sizov, O. S., & Safonov, Y. S. (2018). Rastitel`nye soobshhestva eolovyh form rel`efa severnoj tajgi Zapadnoj sibiri i rekomendacii k rekul`tivacii ogolennyh peskov [Plant Communities of Aeolian Landforms of the Northern Taiga of Western Siberia and Recommendations for the Reclamation of Bare Sands]. Man and the North. In *Proceedings of the XXI All-Russian Scientific and Practical Conference* (pp. 531–535). Pechatnik.

Maslakov, A. A., Egorov, E. G., Zelensky, G. M., Vasil'chuk, Y. K., & Budantseva, N. A. (2021, June 14–18). *The Transient Layer of Permafrost of the Eastern Chukotka Coastal Plains, NE Russia*. Proceedings of the 26th International Conference on Port and Ocean Engineering under Arctic Conditions. Moscow, Russia. https://www.poac.com/Proceedings/2021/POAC21-049.pdf

Maslakov, A. A., Nyland, K. E., Komova, N. N., Yurov, F. D., Yoshikawa, K., & Kraev, G. N. (2020). Community Ice Cellars In Eastern Chukotka: Climatic And Anthropogenic Influences On Structural Stability. *Geography, Environment, Sustainability*, *13*(3), 49–56. https://doi.org/10.24057/2071-9388-2020-71

Maslakov, A., Shabanova, N., Zamolodchikov, D., Volobuev, V., & Kraev, G. (2019). Permafrost Degradation within Eastern Chukotka CALM Sites in the 21st Century Based on CMIP5 Climate Models. *Geosciences, 9*(5), Article 232. https://doi.org/10.3390/geosciences9050232

Maslakov, A., Zotova, L., Komova, N., Grishchenko, M., Zamolodchikov, D., & Zelensky, G. (2021). Vulnerability of the Permafrost Landscapes in the Eastern Chukotka Coastal Plains to Human Impact and Climate Change. *Land, 10*(5), Article 445. https://doi.org/10.3390/land10050445

Mikhailov, I. S. (2020). Changes in the soil-plant cover of the high Arctic of Eastern Siberia. *Eurasian Soil Science, 53*(6), 715–723. https://doi.org/10.1134/S1064229320060083

Moskalenko, N. G., Jorgenson, T., Kanevsky, M., Nossov, D., & Shur, Yu L. (2014). Vzaimosvyazi rastitel'nosti i sezonnogo protaivaniya mnogoletnemerzlyh porod v arcticheskyx tundrah Yamala I Alyaski [The comparative analysis of vegetation and permafrost in arctic tundras of Yamal and Alaska]. *Proceedings of the Russian Geographical Society, 146(3)*, 64–79. https://izv.rgo.ru/jour/article/view/396/214

Myers-Smith, I. H., Hik, D. S., Kennedy, C., Cooley, D., Johnstone, J. F., Kenney, A. J., & Kreb, C. J. (2011). Expansion of Canopy-Forming Willows Over the Twentieth Century on Herschel Island, Yukon Territory, Canada. *AMBIO, 40*(6), 610–623. https://doi.org/10.1007/s13280-011-0168-y

Nelson, F. E., & Outcalt, S. I. (1987). A Computational Method for Prediction and Regionalization of Permafrost. *Arctic and Alpine Research, 19*(3), 279–288. https://doi.org/10.1080/00040851.1987.12002602

Noetzli, J., Christiansen, H., Hrbáček, F., Hu, G., Isaksen, K., Magnin, F., Pogliotti, P., Smith, S. L., Zhao, L., & Streletskiy, D. A. (2023). Permafrost temperature and active layer thickness. *Bulletin of the American Meteorological Society, 104*(9), 39–41. https://doi.org/10.1175/2023BAMSStateoftheClimate.1

O'Neill, H., Smith, S. L., Burn, C., Duchesne, C., & Zhang, Y. (2023). Widespread Permafrost Degradation and Thaw Subsidence in Northwest Canada. *Journal of Geophysical Research: Earth Surface, 128*(8), Article e2023JF007262. https://doi.org/10.1029/2023JF007262

Painter, S. L., Coon, E. T., Khattak, A. J., & Jastrow, J. D. (2023). Drying of tundra landscapes will limit subsidence-induced acceleration of permafrost thaw. *Proceedings of the National Academy of Sciences of the United States of America, 120*(8), Article e2212171120. https://doi.org/10.1073/pnas.2212171120

Rantanen, M., Karpechko, A. Y., Lipponen, A., Nordling, K., Hyvärinen, O., Ruosteenoja, K., Vihma, T., & Laaksonen, A. (2022). The Arctic has warmed nearly four times faster than the globe since 1979. *Communications Earth & Environment*, *3*, Article 168. https://doi.org/10.1038/s43247-022-00498-3

Raynolds, M. K., Walker, D. A., Balser, A., Bay, C., Campbell, M., Cherosov, M. M., Daniëls, F. J., Eidesen, P. K., Ermokhina, K. A., Frost, G. V., Jedrzejek, B., Jorgenson, M. T., Kennedy, B. E., Kholod, S. S., Lavrinenko, I. A., Lavrinenko, O. V., Magnússon, B., Matveyeva, N. V., Metúsalemsson, S., . . . Troeva, E. (2019). A Raster Version of the Circumpolar Arctic Vegetation Map (CAVM). *Remote Sensing of Environment*, *232*, Article 111297. https://doi.org/10.1016/j.rse.2019.111297

Stow, D. A., Hope, A., McGuire, D., Verbyla, D., Gamon, J., Huemmrich, F., Houston, S., Racine, C., Sturm, M., Tape, K., Hinzman, L., Yoshikawa, K., Tweedie, C., Noyle, B., Silapaswan, C., Douglas., D., Griffith, B., Jia, G., Epstein, H., . . . & Myneni, R. (2004). Remote sensing of vegetation and land-cover change in Arctic Tundra Ecosystems. *Remote Sensing of Environment, 89*(3), 281–308. https://doi.org/10.1016/j.rse.2003.10.018

Strand, S. M., Christiansen, H. H., Johansson, M., Åkerman, J., & Humlum, O. (2021). Active layer thickening and controls on interannual variability in the Nordic Arctic compared to the circum-Arctic. *Permafrost and Periglacial Processes, 32*(1), 47–58. https://doi.org/10.1002/ppp.2088

Tishkov, A. A., & Krenke, A. N. (2015). "Pozelenenie" Arktiki v XXI veke kak effekt sinergizma dejstviya global`nogo potepleniya i xozyajstvennogo osvoeniya ["Greening" of the Arctic in the twenty-first century as a synergy effect of global warming and economic development]. *Arctic: Ecology and Economy, 20*(4), 28–37. https://shorturl.at/ZuJUE

Tishkov, A. A., Osokin, N. I., & Sosnovsky, A. V. (2013). Vliyanie sinuzij moxoobraznyh na deyatel'nyj sloj arcticheskyh pochv [The Impact of Moss Synusia on the Active Layer of Arctic Soil and Subsoil]. *Izvestiya Rossiiskoi Akademii Nauk. Seriya Geograficheskaya, 3,* 39–47. https://doi.org/10.15356/0373-2444-2013-3-39-46

Titkova, T. B., & Vinogradova, V. V. (2015). Otklik rastitel`nosti na izmenenie klimaticheskih uslovij v boreal`nyh i subarkticheskih landshaftah v nachale XXI veka [The response of vegetation to climate change in boreal and subarctic landscapes at the beginning of the XXI century]. *Current Problems in Remote Sensing of the Earth from Space, 12*(3), 75–86. http://d33.infospace.ru/\d33_conf/sb2015t3/75-86.pdf

Tyrtikov, A. P. (1969). *Vliianie rastitelnogo pokrova na promerzanie i protaivanie gruntov* [Influence of vegetation cover on freezing and thawing of soils]. Moscow University Press.

Valentini, R., Zamolodchikov, D., Reyer, C., Nose, S., Santini, M., & Lindren, M. (2020). Climate change in Russia — past, present and future. In P. Leskinen, M. Lindner, P. J. Verkerk, G.-J. Nabuurs, J. Van Brusselen, E. Kulikova, M. Hassegawa, & B. Lerink (Eds.), *Russian forests and climate change. What science can tell us* (pp. 45–52). European Forest Institute. https://doi.org/10.36333/wsctu11

Varlamova, E. V., & Soloviev, V. S. (2012). Monitoring rastitel`nogo pokrova arkticheskoj zony Vostochnoj Sibiri po sputnikovym dannym [Monitoring of vegetation cover of the Arctic zone of Eastern Siberia based on satellite data]. *Nauka i obrazovanie, 2*, 58–62. https://cyberleninka.ru/article/n/monitoring-rastitelnogo-pokrova-arkticheskoy-zony-vostochnoy-sibiri-po-sputnikovym-dannym

Vasil'chuk, Y. K., Maslakov, A. A., Budantseva, N. A., Vasil'chuk, A. C., & Komova, N. N. (2021). Isotope Signature Of The Massive Ice Bodies On The Northeast Coast Of Chukotka Peninsula. *Geography, Environment, Sustainability, 4*(14), 9–19. https://doi.org/10.24057/2071-9388-2021-020

Wang, Z., Xiao, M., Nicolsky, D., Romanovsky, V., McComb, C., & Farquharson, L. (2023). Arctic coastal hazard assessment considering permafrost thaw subsidence, coastal erosion, and flooding. *Environmental Research Letters, 18*(10), Article 104003. https://doi.org/10.1088/1748-9326/acf4ac

Yang, Y., Wang, X., & Wang, T. (2024). Permafrost Degradation Induces the Abrupt Changes of Vegetation NDVI in the Northern Hemisphere. *Earth's Future, 12*(10), Article e2023EF004309. https://doi.org/10.1029/2023EF004309

Zamolodchikov, D. G., Kotov, A. N., Karelin, D. V., & Razzhivin, V. Y. (2004). Active-Layer Monitoring in Northeast Russia: Spatial, Seasonal, and Interannual Variability. *Polar Geography, 28*(4), 286–307. https://doi.org/10.1080/789610207

Zhiltsova, E. L., & Anisimov, O. A. (2013). Empiriko-statisticheskoe modelirovanie rastitel`noj zonal`nosti v usloviyah izmeneniya klimata na territorii Rossii [Empirico-statistical modeling of vegetation zonation under climate change in Russia]. *Problems of Ecological Monitoring and Ecosystems Modeling*, *25*, 360–374. https://www.rosih.ru/shop/1451091132.pdf

Appendix

Table 1a. The seasons of vegetation activity peak for 2000–2023 based on NDVI information

Year	Vegetation activity peak	Source
2000	July 20–25	NOAA CDR
2001	July 30–August 04	NOAA CDR
2002	July 23–29	eModis NDVI V6
2003	July 30–August 05	eModis NDVI V6
2004	July 15–21	eModis NDVI V6
2005	July 23–29	eModis NDVI V6
2006	August 06–12	eModis NDVI V6
2007	August 13–19	eModis NDVI V6
2008	August 05–11	eModis NDVI V6
2009	August (06) 13–19	eModis NDVI V6
2010	August 13–19	eModis NDVI V6
2011	July 30–August 05	eModis NDVI V6
2012	July 22–28	eModis NDVI V6
2013	July 23–29	eModis NDVI V6
2014	July 30–August 06	eModis NDVI V6
2015	July 23–29	eModis NDVI V6
2016	July 29–August 04	eModis NDVI V6
2017	July 30–August 05	eModis NDVI V6
2018	July 23–29	eModis NDVI V6
2019	July 30–August 05	eModis NDVI V6
2020	July 22–28	eModis NDVI V6
2021	July 30–August 05	eModis NDVI V6
2022	July 30–August 05	eVIIRS
2023	August 13–19	eVIIRS

Table 2a. Landsat satellite images for ECCP for July and August of 2000–2023 selected for the study

Year	Total number of images for July–August	Number of cloudless images for July–August	Selected images	
			Date of the image	Source
2000	10	2	17.07.2000	Landsat-7
2001	9	1 (+2 with light cloud cover throughout)	05.08.2001	Landsat-7
2002	9	2 (+1 with light cloud cover throughout)	23.07.2002	Landsat-7
2003	6	1	27.08.2003	Landsat-7
2004	12	5	26.07.2004	Landsat-7
2005	10	6	29.07.2005	Landsat-7
2006	21	5	24.07.2006	Landsat-5
2007	25	7	21.08.2007	Landsat-5
2008	11	5	08.08.2008	Landsat-7
2009	7	2	09.08.2009	Landsat-5
2010	10	1	22.08.2010*	Landsat-7
2011	18	2	15.08.2011	Landsat-7
2012	8	2	09.07.2012*	Landsat-7
2013	23	2	13.07.2013*	Landsat-8
2014	17	1 (partly with clouds)	07.07.2014*	Landsat-8

Table 2a. Landsat satellite images for ECCP for July and August of 2000–2023 selected for the study (*continued*)

Year	Total number of images for July–August	Number of cloudless images for July–August	Selected images	
			Date of the image	Source
2015	21	4	02.08.2015	Landsat-8
2016	20	6	04.08.2016	Landsat-8
2017	19	1 (partly with clouds)	24.07.2017	Landsat-8
2018	19	2	25.07.2018	Landsat-8
2019	18	4	06.08.2019	Landsat-8
2020	19	1	08.08.2020*	Landsat-8
2021	23	3 (+1 with light cloud cover throughout)	04.08.2021	Landsat-8
2022	37	2	28.07.2022	Landsat-9
2023	37	3	09.08.2023	Landsat-9

Note. Data marked with an asterisk (*) are attributed to the dates differing from the vegetation peak by more than 6 days.

Table 3a. Results NDVI calculations based on Landsat satellite images for 2001–2023 for the ECCP key area

Year	Cloudness (%)	Average NDVI	Median NDVI	Standard deviation NDVI
2000	66.00	.39	.43	.14
2001	1.00	.06*	.05*	.04*
2002	35.00	.45	.50	.15
2003	50.00	.39	.44	.13
2004	18.00	.36	.40	.18
2005	6.00	.46	.52	.15
2006	0.00	.44	.49	.15
2007	23.00	.41	.46	.14
2008	6.00	.43	.47	.14
2009	2.00	.42	.48	.15
2010	20.00	.42	.48	.15
2011	33.00	.47	.53	.16
2012	3.00	.41	.45	.13
2013	50.00	.39	.42	.16
2014	47.11	.36	.40	.15
2015	44.47	.52	.58	.15
2016	1.62	.51	.57	.15
2017	86.53	.05*	.05*	.02*
2018	32.82	.42	.49	.17
2019	50.74	.52	.59	.16
2020	89.84	.49	.56	.18
2021	15.70	.51	.56	.15
2022	82.33	.41	.46	.16
2023	65.94	.43	.49	.18

Note. Data marked with an asterisk (*) are attributed to the images with a significant proportion of cloudiness.